$\alpha(m_Z^2)$ FROM LATTICE QCD AND IMPLICATIONS

Marco Cè Antoine Gérardin Georg von Hippel Ben Hörz
Renwick J. Hudspith Simon Kuberski Harvey B. Meyer Kohtaroh Miura
Daniel Mohler Konstantin Ottnad Srijit Paul Andreas Risch
Teseo San José Jonas Wilhelm Hartmut Wittig

Electroweak Precision Physics from Beta Decays to the Z pole
Mainz Institute for Theoretical Physics, Johannes Gutenberg University
24-28 October 2022

The electromagnetic coupling

An interesting quantity...

- $\alpha(m_Z^2)$ enters the electroweak global fits of the Standard Model [1]

$$m_H = 91^{+18}_{-16}\ \text{GeV}$$

- Using the parametrisation

$$\alpha(Q^2) = \frac{\alpha}{1 - (\Delta\alpha)_{\text{lep}}(Q^2) - (\Delta\alpha)_{\text{had}}(Q^2)\ldots}$$

  a_μ^{HVP} and $(\Delta\alpha)_{\text{had}}$ can be related in the space-like region $\rightarrow$ **changes to a_μ^{HVP} may affect m_H through $\alpha(m_Z^2)$**

... to compute on the lattice

- The hadronic contribution dominates the uncertainty:

$$(\Delta\alpha)_{\text{lep}}(m_Z^2) = 314.979(2) \times 10^{-4} \quad [2, 3]$$

$$(\Delta\alpha)^{(5)}_{\text{had}}(m_Z^2) = 276.09(112) \times 10^{-4} \quad [4]$$

$$(\Delta\alpha)^{(t)}_{\text{had}}(m_Z^2) = -0.7201(37) \times 10^{-4} \quad [4]$$

Compute $(\Delta\alpha)^{(5)}_{\text{had}}(m_Z^2)$

Method 1: Dispersion relation (DR)

$$(\Delta\alpha)^{(5)}_{\text{had}}(Q^2) = -\frac{\alpha Q^2}{3\pi} P \int_{m_\pi^2}^{\infty} \mathrm{d}s \, \frac{R(s)}{s(s-Q^2)} \leftarrow \text{ for } Q^2 = m_Z^2$$

where for the R-ratio one uses the experimental data

$$R(Q^2) \equiv \frac{\sigma_{\text{total}}\left(e^+e^- \to \text{hadrons}\right)}{\sigma\left(e^+e^- \to \mu^+\mu^-\right)}$$

up to certain energy, and then switches to perturbation theory.

Method 2: Adler function approach, aka "Euclidean split technique" [5, 6, 7, 8]

$$\begin{aligned}(\Delta\alpha)^{(5)}_{\text{had}}(m_Z^2) = {} & (\Delta\alpha)^{(5)}_{\text{had}}(-Q_0^2) \leftarrow \text{ LQCD or DR for } Q^2 = -Q_0^2 \\ & + \left((\Delta\alpha)^{(5)}_{\text{had}}(-m_Z^2) - (\Delta\alpha)^{(5)}_{\text{had}}(-Q_0^2)\right) \leftarrow \text{ pQCD or DR} \\ & + \left((\Delta\alpha)^{(5)}_{\text{had}}(m_Z^2) - (\Delta\alpha)^{(5)}_{\text{had}}(-m_Z^2)\right) \leftarrow \text{ pQCD}\end{aligned}$$

Slide taken from Hartmut Wittig's Lattice 2022 talk

Inputs to the Adler function approach

First term: Lattice result for $(\Delta\alpha)^{(5)}_{\text{had}}(-Q_0^2)$ for $Q_0^2 = 3$ to $7\,\text{GeV}^2$

Second term: The Adler function

$$D(-Q^2) = \frac{3\pi}{\alpha} Q^2 \frac{\mathrm{d}(\Delta\alpha)^{(5)}_{\text{had}}(Q^2)}{\mathrm{d}Q^2}$$

It is known to three loops in pQCD → Jegerlehner's **pQCDAdler** package

$$\left[(\Delta\alpha)^{(5)}_{\text{had}}(-m_Z^2) - (\Delta\alpha)^{(5)}_{\text{had}}(-Q_0^2)\right]_{\text{pQCD/Adler}} = \frac{\alpha}{3\pi}\int_{Q_0^2}^{m_Z^2} \frac{\mathrm{d}Q^2}{Q^2} D(Q^2)$$

The result depends on Q_0^2

Third term: Perturbation theory [9]

$$\left[(\Delta\alpha)^{(5)}_{\text{had}}(m_Z^2) - (\Delta\alpha)^{(5)}_{\text{had}}(-m_Z^2)\right]_{\text{pQCD}} = 0.000\,045(2)$$

Slide taken from Hartmut Wittig's Lattice 2022 talk

Time-momentum representation

As a function of the momentum exchanged $Q^2 > 0$,

$$\alpha(-Q^2) = \frac{\alpha}{1 - (\Delta\alpha)_{\mathrm{lep}}(-Q^2) - (\Delta\alpha)_{\mathrm{had}}(-Q^2)\dots}$$

The leading hadronic contribution is written in terms of the vacuum polarisation tensor

$$\Pi^{\gamma\gamma}_{\mu\nu}(Q) = \int \mathrm{d}^4x \; e^{iQx} \left\langle V^{\gamma}_{\mu}(x) V^{\gamma}_{\nu}(0) \right\rangle_{\mathrm{QCD}}$$

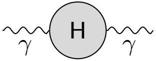

Then, the time-momentum representation [10, 11] of the coupling reads

$$(\Delta\alpha)_{\mathrm{had}}(-Q^2) = 4\pi\alpha \; \bar{\Pi}^{\gamma\gamma}(-Q^2) \qquad \bar{\Pi}^{\gamma\gamma}(-Q^2) = \int_0^{\infty} \mathrm{d}t \; G^{\gamma\gamma}(t) K(t, Q^2)$$

where $\bar{\Pi}(-Q^2) = \Pi(-Q^2) - \Pi(0)$.
The piece that we compute on the lattice is

$$G^{\gamma\gamma}(t) = -\frac{a^3}{3} \sum_{k=1}^{3} \sum_{\vec{x}} \left\langle V^{\gamma}_{k}(x) V^{\gamma}_{k}(0) \right\rangle_{\mathrm{QCD}}$$

The vector current V_k^γ

- The electromagnetic current is

$$V_k^\gamma = 2/3\bar{u}\gamma_k u - 1/3\bar{d}\gamma_k d + 2/3\bar{c}\gamma_k c - 1/3\bar{s}\gamma_k s,$$

- The isospin decomposition is very convenient,

$$V_k^\gamma = V_k^3 + 1/\sqrt{3}V_k^8 + 2/3V_k^c$$

- In terms of the quark flavours computed on the lattice,

Iso-vector,	$V_k^3 = 1/2(\bar{u}\gamma_k u - \bar{d}\gamma_k d)$
Iso-scalar,	$V_k^8 = 1/(2\sqrt{3})(\bar{u}\gamma_k u + \bar{d}\gamma_k d - 2\bar{s}\gamma_k s)$

- We use two V_k discretisations: local and conserved

$$(V_k^a)^{\mathrm{L}} = \bar{\psi}(x)\gamma_k\lambda^a/2\psi(x)$$

$$(V_k^a)^{\mathrm{C}} = 1/2\left(\bar{\psi}(x+a\hat{k})(1+\gamma_k)U_k^\dagger(x)\lambda^a/2\psi(x) - \bar{\psi}(x)(1-\gamma_k)U_k(x)\lambda^a/2\psi(x+a\hat{k})\right)$$

Coordinated lattice simulations (CLS)

- $N_f = 2+1$ $\mathcal{O}(a)$-improved Wilson action
- Tree-level improved Lüscher-Weisz action
- Periodic/open temporal boundary conditions
- Chiral trajectory $m_\pi^2/2 + m_K^2 \approx$ const
- Pion masses $130\,\text{MeV} < m_\pi < 420\,\text{MeV}$
- $a = (50,\ 64,\ 76 \text{ and } 86) \times 10^{-3}\text{fm}$
- Volumes $m_\pi L > 4$
- Local and conserved discretisations
- Use the scale $\sqrt{8t_0}$ [12] or af_π [13]

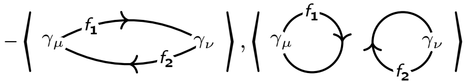

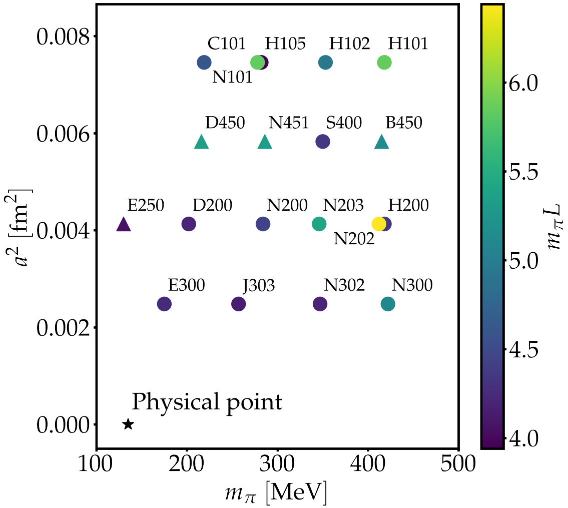

[14, 12]

Sources of uncertainty

To produce highly accurate results, our analysis needs to study the following topics:

- Signal-to-noise ratio
- Finite box size
- Finite lattice spacing
- Unphysical quark masses
- Scale setting
- Isospin breaking effects (quark-connected component estimated in subset of ensembles)
- Missing sea charm and bottom quarks (insignificant [15, 16])

Signal-to-noise ratio

- Bounding method: The isovector G^{33} and isoscalar G^{88} components fulfil

$$0 \leq G(t_{\rm cut})e^{-m_{\rm eff}(t)(t-t_{\rm cut})} \leq G(t) \leq G(t_{\rm cut})e^{-E_0(t-t_{\rm cut})}, \qquad t \geq t_{\rm cut} \text{ [16]}$$

Example at physical m_π:

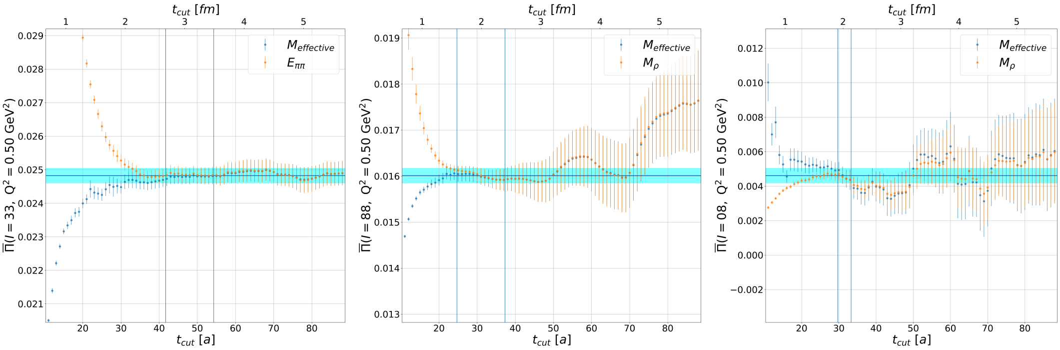

Finite box size

Correct the isovector correlator for finite-size effects

$$G^{33}(t,\infty) = G^{33}(t,L) + \Delta G^{33}(t,L) \qquad \Delta G^{33}(t,L) = G^{33}_{\text{model}}(t,\infty) - G^{33}_{\text{model}}(t,L)$$

At small distances, where many-pion interactions are important, we apply the Hansen-Patella (HP) method [17, 18]

- It expands $\Delta G^{33}(t,L)$ in the pion winding number
- We use the space-like pion form-factor

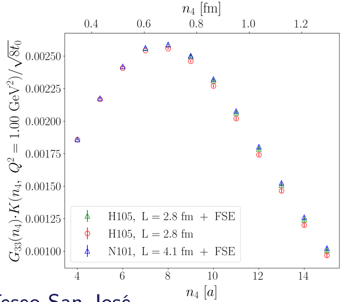

At large distances, where the $\pi\pi$ state dominates, we can also use the Meyer-Lellouch-Lüscher (MLL) method [19, 11, 20, 21]

- Models $G^{33}_{\text{model}}(t,L)$ and $G^{33}_{\text{model}}(t,\infty)$ separately
- We use the time-like pion form-factor

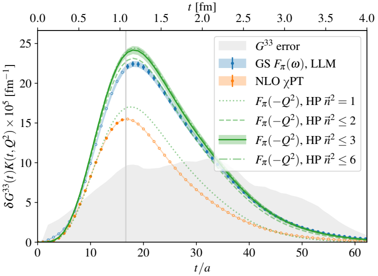

Finite lattice spacing and unphysical quark masses

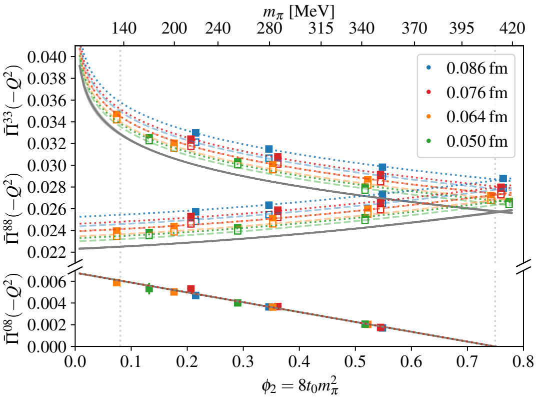

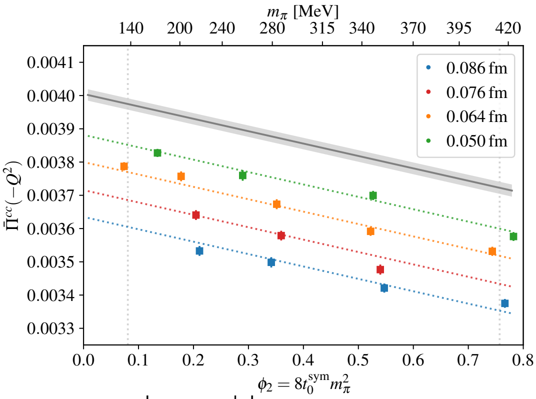

$$(\Delta\alpha)_{\mathsf{had}}(-1\,\mathrm{GeV}^2)\times 10^6 = 3864\ \underbrace{(17)}_{\text{Statistical}}\ \underbrace{(8)}_{\text{Extrapolation}}\ \overbrace{(22)}^{\text{Scale setting}}\ \overbrace{(4)}^{\text{charm-quark loops}}\ \underbrace{(12)}_{\text{Isospin breaking}}\ [\overbrace{32}^{\text{Total}},\ \underbrace{0.8\,\%}_{\text{Percentage}}]$$

$\bar{\Pi}$ vs Q^2

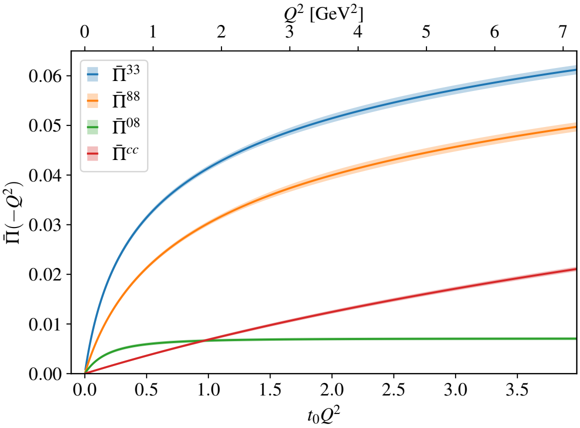

Use Padé Ansätze for $Q^2 \leq 7\,\text{GeV}$

$$\bar{\Pi} = \left(\sum_{n=1}^{N} a_n Q^{2n} \right) \Big/ \left(1 + \sum_{m=1}^{M} b_m Q^{2m} \right)$$

$(\Delta\alpha)_{\text{had}}$ at low momentum, comparison

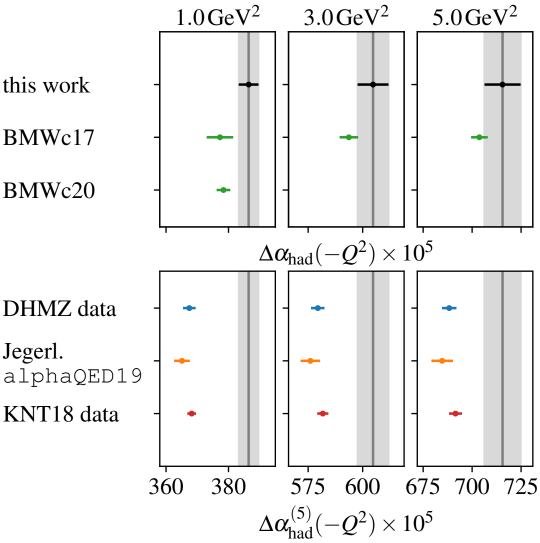

$(\Delta\alpha)_{\mathrm{had}}$ at the Z pole, comparison

Mainz/CLS $\quad (\Delta\alpha)_{\mathrm{had}}(m_Z^2) = 0.027\,73(15)$
(lattice input + pQCD/Adler)

Jegerlehner 19 $\quad (\Delta\alpha)_{\mathrm{had}}(m_Z^2) = 0.027\,53(12)$
(R-ratio input + pQCD/Adler)

- The indirect determination of the Higgs mass is affected [22]:

$$m_H = 91^{+18}_{-16}\text{ GeV} \quad \rightarrow \quad m_H = 78^{+?}_{-?}\text{ GeV}$$

- The agreement within errors at the Z-pole doesn't erase the tension for low Q^2

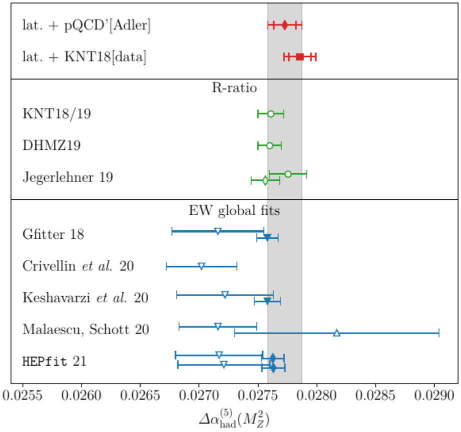

▽ Leaving $(\Delta\alpha)_{\mathrm{had}}(m_Z^2)$ as a free parameter

△ Leaving $(\Delta\alpha)_{\mathrm{had}}(m_Z^2)$ and m_H as free parameters

▼ ♦ As ▽, but using priors for $(\Delta\alpha)_{\mathrm{had}}(m_Z^2)$ centred around the R-ratio/BMWc estimate

Slide taken from Hartmut Wittig's Lattice 2022 talk

Relative contributions to $(\Delta\alpha)^{(5)}_{\mathrm{had}}(m_Z^2)$

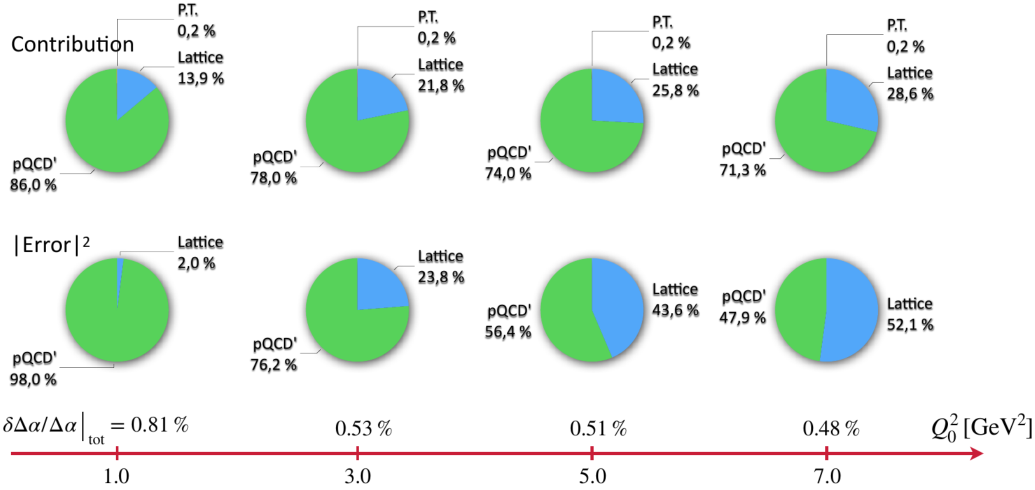

Slide taken from Hartmut Wittig's Lattice 2022 talk

Implications for other quantities

The R-ratio uses experimental data

$$R(Q^2) \equiv \frac{\sigma_{\text{total}}\left(e^+e^- \to \text{hadrons}\right)}{\sigma\left(e^+e^- \to \mu^+\mu^-\right)}$$

It gives access to the process

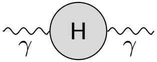

With this diagram, we can compute the QCD contribution to several quantities:

$$a_\mu \qquad \alpha(Q^2) \qquad \sin^2\theta_W(Q^2)$$

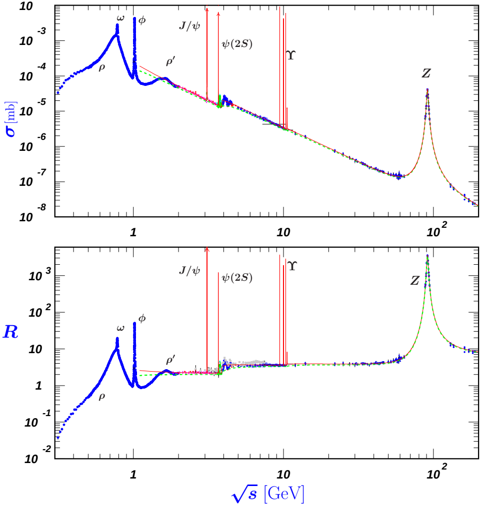

[22]

The hadronic vacuum polarisation contribution to the muon $g-2$

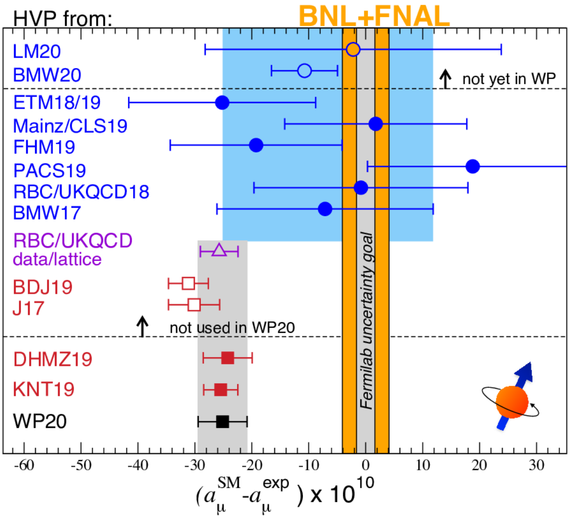

Slide taken from Simon Kuberski's Lattice 2022 talk

← a_μ^{HVP} status [23]

- BMW20 prediction [24] has similar precision to phenomenology, but it deviates from data-driven results
- We need more precise lattice determinations. Challenging systematics:
  - At short distances, cut-off effects
  - At long distances, noise
- For a clear comparison between lattice determinations → Use time windows in the TMR as benchmarks [25]

Time-momentum representation

Intermediate Euclidean time window of a_μ^{HVP}:

$$a_\mu^{\mathrm{win}} \equiv \left(\frac{\alpha}{\pi}\right)^2 \int_0^\infty \mathrm{d}t\ \tilde{K}(t) G^{\gamma\gamma}(t) \left[\Theta(t, t_0, \Delta) - \Theta(t, t_1, \Delta)\right]$$

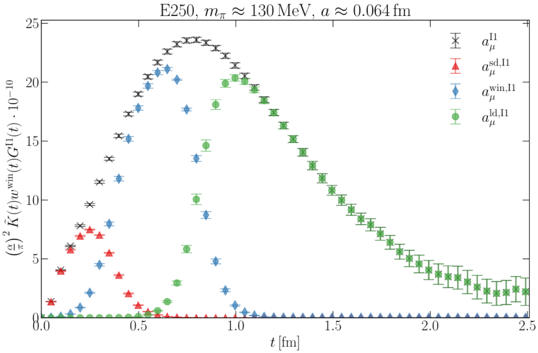

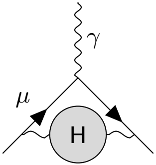

$$G^{\gamma\gamma}(t) = -\frac{a^3}{3} \sum_{k=1}^{3} \sum_{\vec{x}} \left\langle V_k^\gamma(x) V_k^\gamma(0) \right\rangle_{\mathrm{QCD}}$$

$$\Theta(t, t', \Delta) \equiv \frac{1}{2}\left(1 + \tanh[(t - t')/\Delta]\right)$$

$$t_0 = 0.4\,\mathrm{fm}, \quad t_1 = 1.0\,\mathrm{fm}, \quad \Delta = 0.15\,\mathrm{fm}$$

Intermediate window:

- Cut-off effects are suppressed
- No noise problem
- Per-mil uncertainty

Slide taken from Simon Kuberski's Lattice 2022 talk

Comparing a_μ^{win} with the R-ratio

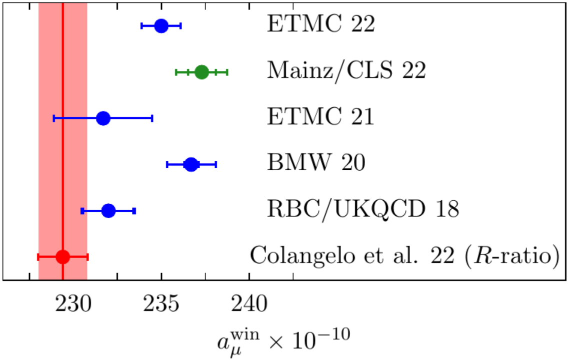

- $3.9\,\sigma$ tension with data-driven estimate [26]
- Need to look at the other windows

The electroweak mixing $\sin^2\theta_W$

The electroweak mixing angle is defined as

$$\sin^2\theta_W = \frac{\alpha}{\alpha_2}$$

where $4\pi\alpha = e^2$, $4\pi\alpha_2 = g^2$, g the $SU(2)_L$ coupling

The standard theory approach separates the quark flavour components of the R-ratio → the lattice avoids this systematic

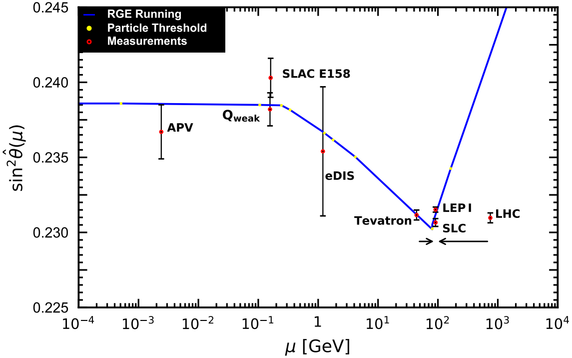

Experiments MOLLER [27] and SoLID [28] at JLAB, and P2 [29] in Mainz University → Precision in the range 0.15 % to 1 % at low energy μ

Time-momentum representation

As a function of the momentum exchanged $Q^2 > 0$,

$$\alpha(-Q^2) = \frac{\alpha}{1 - \Delta\alpha(-Q^2)}, \qquad \sin^2\theta_W(-Q^2) = \sin^2\theta_W\left(1 + \Delta\sin^2\theta_W(-Q^2)\right)$$

where $(\Delta\sin^2\theta_W)_{\text{had}}(-Q^2) \equiv (\Delta\alpha)_{\text{had}}(-Q^2) - (\Delta\alpha_2)_{\text{had}}(-Q^2)$
The leading hadronic contributions are related to two subtracted vacuum polarisation functions:

$$(\Delta\alpha)_{\text{had}}(-Q^2) = 4\pi\alpha\ \bar{\Pi}^{\gamma\gamma}(-Q^2), \qquad (\Delta\sin^2\theta_W)_{\text{had}}(-Q^2) = -\frac{4\pi\alpha}{\sin^2\theta_W}\ \bar{\Pi}^{Z\gamma}(-Q^2)$$

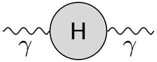

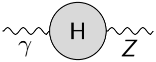

Use the time-momentum representation [10, 11] to express the subtracted vacuum polarisation function

$$\bar{\Pi}^{\gamma\gamma}(-Q^2) = \int_0^\infty \mathrm{d}t\ G^{\gamma\gamma}(t)K(t,Q^2), \qquad \bar{\Pi}^{Z\gamma}(-Q^2) = \int_0^\infty \mathrm{d}t\ G^{Z\gamma}(t)K(t,Q^2),$$

$$G^{Z\gamma}(t) = -\frac{a^3}{3}\sum_{k=1}^{3}\sum_{\vec{x}}\left\langle V_k^Z(x)V_k^\gamma(0)\right\rangle_{\text{QCD}}$$

The vector currents V_k^γ, V_k^Z

- The two basic currents are

$$V_k^\gamma = \frac{2}{3}\bar{u}\gamma_k u - \frac{1}{3}\bar{d}\gamma_k d + \frac{2}{3}\bar{c}\gamma_k c - \frac{1}{3}\bar{s}\gamma_k s, \qquad V_k^{T_3} = \frac{1}{4}\bar{u}\gamma_k u - \frac{1}{4}\bar{d}\gamma_k d + \frac{1}{4}\bar{c}\gamma_k c - \frac{1}{4}\bar{s}\gamma_k s$$

- An isospin decomposition is very convenient,

$$V_k^\gamma = V_k^3 + 1/\sqrt{3}V_k^8 + 2/3V_k^c$$
$$V_k^Z = V_k^{T_3} - \sin^2\theta_W V_k^\gamma = (1/2 - \sin^2\theta_W)V_k^\gamma - 1/6V_k^0 - 1/12V_k^c$$

- In terms of the quark flavours,

Iso-vector,	$V_k^3 = 1/2(\bar{u}\gamma_k u - \bar{d}\gamma_k d)$
Iso-scalar,	$V_k^8 = 1/(2\sqrt{3})(\bar{u}\gamma_k u + \bar{d}\gamma_k d - 2\bar{s}\gamma_k s)$
Iso-singlet,	$V_k^0 = 1/2(\bar{u}\gamma_k u + \bar{d}\gamma_k d + \bar{s}\gamma_k s)$

- We use two V_k discretisations: local and conserved

$$(V_k^a)^{\mathrm{L}} = \bar{\psi}(x)\gamma_k\lambda^a/2\psi(x)$$
$$(V_k^a)^{\mathrm{C}} = 1/2\left(\bar{\psi}(x+a\hat{k})(1+\gamma_k)U_k^\dagger(x)\lambda^a/2\psi(x) - \bar{\psi}(x)(1-\gamma_k)U_k(x)\lambda^a/2\psi(x+a\hat{k})\right)$$

$(\Delta\alpha_2)_{\text{had}}$ at low momentum, comparison

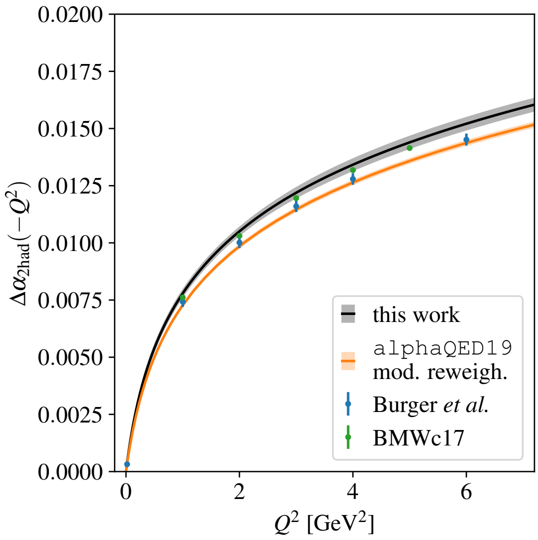

Summary and Outlook

- Lattice+pQCD/Adler estimate for $(\Delta\alpha)_{\text{had}}(m_Z^2)$ broadly agrees with global electroweak fits $\rightarrow$ no contradiction with the Standard Model here
- Standard Model can accommodate a larger value for a_μ without contradicting electroweak precision data
- Our result for a_μ^{win}, $(\Delta\alpha)_{\text{had}}(-Q^2)$ and $(\Delta\sin^2\theta_W)_{\text{had}}(-Q^2)$ are in tension with the R-ratio $\rightarrow 3\,\sigma$ to $5\,\sigma$

An update of the 2019 determination of a_μ^{HVP} is ongoing:

- Investigate other time windows
- Reduce statistical errors
- Improve the scale setting
- Extend isospin breaking (IB) calculations to more ensembles

For a detailed explanation, see

- arXiv:2203.08676
- arXiv:2206.06582

$\mathcal{O}(a)$ improved and renormalised vector currents

- Use the tensor current $\Sigma^a_{\mu\nu}$ for $\mathcal{O}(a)$ improvement [30, 31],

$$(V^a_k)^\alpha_{\mathrm{I}}(x) = (V^a_k)^\alpha(x) + ac^\alpha_V(g_0)\tilde{\partial}_\nu \Sigma^a_{\mu\nu}(x), \qquad \text{with } \alpha = \mathrm{L}, \mathrm{C}$$

- Renormalisation and mass-dependent improvement of local currents via [30, 31]

$$\left(V^3_k\right)^{\mathrm{L}}_{\mathrm{R}} = Z_V\left(1 + 3\bar{b}_V am^{\mathrm{av}}_q + b_V am_{q,l}\right)\left(V^3_k\right)^{\mathrm{L}}_{\mathrm{I}},$$

$$\begin{pmatrix} V^8_k \\ V^0_k \end{pmatrix}^{\mathrm{L}}_{\mathrm{R}} = Z_V \begin{pmatrix} 1 + 3\bar{b}_V am^{\mathrm{av}}_q + \frac{b_V}{3}(am_{q,l} + 2am_{q,s}) & \left(\frac{b_V}{3} + f_V\right)\frac{2}{\sqrt{3}}(am_{q,l} - am_{q,s}) \\ \frac{r_V d_V}{3}(am_{q,l} - m_{q,s}) & r_V + r_V(3\bar{d}_V + d_V)am^{\mathrm{av}}_q \end{pmatrix} \begin{pmatrix} V^8_k \\ V^0_k \end{pmatrix}^{\mathrm{L}}_{\mathrm{I}}$$

- Two independent non-perturbative determinations of Z_V, c^{L}_V, c^{C}_V, b_V, $\bar{b}_V$

Set 1 Large-volume CLS ensembles [30]

Set 2 Small-volume Schrödinger functional [32, 33] They differ by higher order cut-off effects. f_V is of $\mathcal{O}(g_0^6)$ and unknown

The Γ method vs jackknife binning [34, 14]

Measurements are taken every 4 MDU.
Runs with the same trajectory length should show Langevin scaling, $\bar{\bar{\tau}}_{\bar{\Pi},\mathrm{int}} \propto a^{-2}$. OBC are taking to alleviate the increase in autocorrelations towards the The error estimate using the Γ method includes autocorrelations explicitly,

$$\left(\Delta \bar{\bar{F}}\right)^2 = 2\bar{\bar{\tau}}_{F,\mathrm{int}} \left(\Delta_0 \bar{\bar{F}}\right)^2, \qquad \left(\Delta_{\mathrm{jack}} \bar{F}\right)^2 = \frac{N_B - 1}{N_B} \sum_{k=1}^{N_B} \left(f(c_\alpha^k) - \bar{F}\right)^2.$$

Both methods minimize the total error of the error to find the correct uncertainty,

$$\frac{\Delta_{\mathrm{total}}\left(\Delta \bar{\bar{F}}\right)}{\Delta \bar{\bar{F}}} \approx \frac{1}{2} \min_w \left(e^{-w/\tau_{F,\mathrm{D}}} + 2\sqrt{\frac{w}{N}}\right), \qquad \frac{\Delta_{\mathrm{total}}\left(\Delta_{\mathrm{jack}} \bar{F}\right)}{\Delta_{\mathrm{jack}} \bar{F}} \approx \frac{1}{2} \min_B \left(\frac{\tau_{F,\mathrm{D}}}{B} + \sqrt{\frac{2B}{N}}\right).$$

The systematic error of the error is different,

$$\frac{\Delta_{\mathrm{sys}}\left(\Delta \bar{\bar{F}}\right)}{\Delta_{\mathrm{sta}}\left(\Delta \bar{\bar{F}}\right)} \approx \frac{1}{\log\left(N/\tau_{F,\mathrm{D}}\right)}, \qquad \frac{\Delta_{\mathrm{sys}}\left(\Delta_{\mathrm{jack}} \bar{F}\right)}{\Delta_{\mathrm{sta}}\left(\Delta_{\mathrm{jack}} \bar{F}\right)} = \frac{1}{2}.$$

The systematic error of the error for the Γ method vanishes with increasing statistics.

The Γ method vs jackknife binning [34]

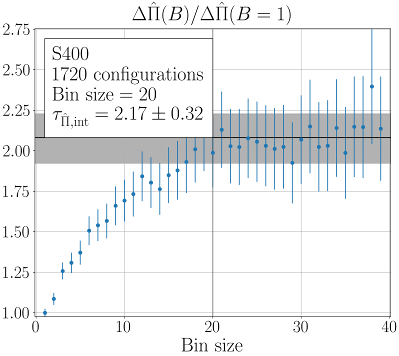

Ensemble S400, with M_π = 351 MeV

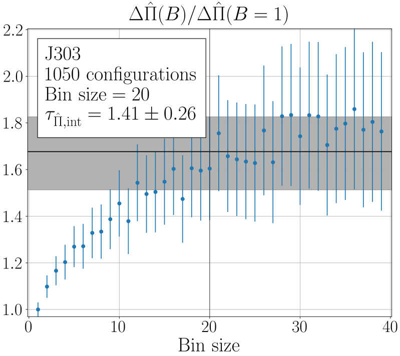

Ensemble J303, with M_π = 257 MeV

The vertical line shows the estimated optimal bin size B, and the horizontal band shows

$$\Delta\bar{\Pi}(B)/\Delta\bar{\Pi}(1) = \sqrt{2\tau_{\bar{\Pi},\mathrm{int}}} = \text{const},$$

which is the expected uncertainty increase when taking into account autocorrelations.

The Γ method vs jackknife binning

CLS	aM_π	Bin size	$\tau_{\bar{\Pi},\mathrm{int}}$
H101	0.1830 (5)	25	1.70 (26)
H102	0.1546 (5)	25	1.73 (27)
H105	0.1234 (13)	20	1.32 (27)
N101	0.1222 (5)	15	0.79 (11)
C101	0.0960 (6)	20	0.79 (10)
B450	0.1605 (4)	25	1.45 (24)
S400	0.1358 (4)	20	2.17 (32)
N451	0.1108 (3)	10	0.73 (10)
D450	0.0836 (4)	5	0.55 (7)
H200	0.1363 (5)	30	1.20 (19)
N202	0.1342 (3)	35	1.86 (45)
N203	0.1124 (2)	20	1.15 (17)
N200	0.0922 (3)	15	0.77 (10)
D200	0.0655 (3)	10	0.58 (6)
E250	0.0422 (2)	5	0.47 (4)
N300	0.1067 (3)	40	3.36 (67)
N302	0.0875 (3)	30	2.07 (33)
J303	0.0649 (2)	20	1.41 (26)
E300	0.0442 (1)	20	1.07 (22)

The pion masses were obtained by the Mainz group using an implementation of the PhD thesis [35]. B and $\tau_{\bar{\Pi},\mathrm{int}}$ are computed using the *Python* code [36].

Time-momentum representation [10, 11]

$$K(t, Q^2) = t^2 - \frac{4}{Q^2} \sin^2\left(\frac{Qt}{2}\right)$$

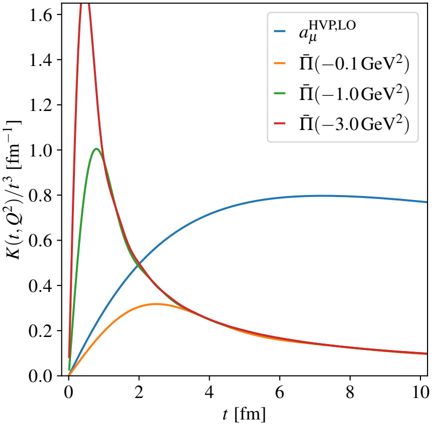

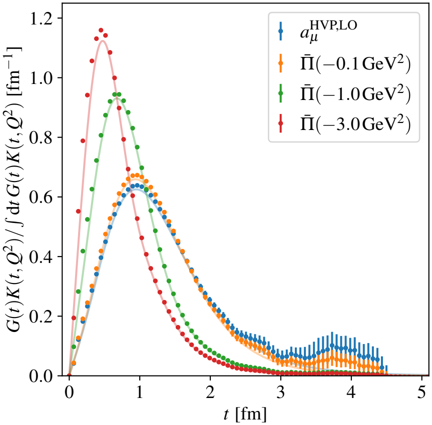

Extrapolation to the physical point

Extrapolate to the isospin-symmetric physical point on the dimensionless variables [12, 22, 37]

$$a^2/8t_0^{\mathrm{sym}} \to 0$$
$$\phi_2 = 8t_0 M_\pi^2 \to \phi_2^{\mathsf{phy}} = 0.0806(17)$$
$$\phi_4 = 8t_0(M_\pi^2/2 + M_k^2) \to \phi_4^{\mathsf{phy}} = 1.124(24)$$

Fit models

$$\begin{aligned}
\bar{\Pi}^{\mathrm{charm}}(a^2/8t_0^{\mathrm{sym}}, \phi_2) &= \bar{\Pi}^{cc,\mathsf{sym}} + \delta_2^d\left(a^2/8t_0^{\mathsf{sym}}\right) + \gamma_1^{cc}\left(\phi_2 - \phi_2^{\mathrm{sym}}\right)\\
\bar{\Pi}^{08}(\phi_2, \phi_4) &= \lambda_1\left(\phi_4 - 3/2\phi_2\right)\\
\bar{\Pi}^{i=33,88}(a^2/8t_0^{\mathrm{sym}}, \phi_2, \phi_4) &= \bar{\Pi}^{\mathrm{sym}} + \gamma_1^i\left(\phi_2 - \phi_2^{\mathrm{sym}}\right) + \eta_1\left(\phi_4 - \phi_4^{\mathrm{sym}}\right)\\
&+ \gamma_2^i \begin{cases} \log\left(\phi_2/\phi_2^{\mathrm{sym}}\right) \\ \left(\phi_2 - \phi_2^{\mathrm{sym}}\right)^2 \end{cases} + \begin{cases} \delta_2^d\left(a^2/8t_0^{\mathsf{sym}}\right) \\ \delta_2^d\left(a^2/8t_0^{\mathsf{sym}}\right) + \delta_3^d\left(a^2/8t_0^{\mathsf{sym}}\right)^{3/2} \end{cases}
\end{aligned}$$

Total least-squares minimisation

We use the Levenberg-Marquardt algorithm [38] as implemented in the SciPy package [39] *least_squares* routine. Different ensembles are uncorrelated,

$$\chi^2 = \sum_e \chi_e^2 \equiv \sum_e \begin{cases} \chi^2_{e,-}, & \text{if } M_{\pi,e} \neq M_{K,e}, \\ 1/2\left(\chi^2_{e,33} + \chi^2_{e,88}\right), & \text{if } M_{\pi,e} = M_{K,e}. \end{cases}$$

The index e runs over the ensembles.

$\chi^2_{e,-}$, $\chi^2_{e,33}$ and $\chi^2_{e,88}$ can be written with the same generic structure $r^T \text{Cov}^{-1} r$, where

- $r = \text{model} - \text{data}$ is the vector of residues.
- Cov is the covariance matrix, whose entries can be computed using

$$\mathrm{Cov}_{e,\cdot}[x,y] = \frac{1}{N_b - 1} \sum_{s=1}^{N_b} \left(x_s - E[x]\right)\left(y_s - E[y]\right),$$

where s runs over the bootstrap samples, of which there are N_b in total.

r and Cov for non-SU(3)$_\mathrm{f}$-symmetric ensembles

The residue vector is defined as

$$r_{e,-} = \begin{pmatrix} \phi_2 \\ \phi_4 \\ \bar{\Pi}(a,\phi_2,\phi_4; d=\mathrm{l}, i=33) \\ \bar{\Pi}(a,\phi_2,\phi_4; d=\mathrm{s}, i=33) \\ \bar{\Pi}(a,\phi_2,\phi_4; d=\mathrm{l}, i=88) \\ \bar{\Pi}(a,\phi_2,\phi_4; d=\mathrm{s}, i=88) \end{pmatrix} - \begin{pmatrix} \phi_2 \\ \phi_4 \\ \bar{\Pi}^{\mathrm{l}}_{33} \\ \bar{\Pi}^{\mathrm{s}}_{33} \\ \bar{\Pi}^{\mathrm{l}}_{88} \\ \bar{\Pi}^{\mathrm{s}}_{88} \end{pmatrix}_e ,$$

where e runs over the ensembles data. The index structure of the covariance matrix is

$$\mathrm{Cov}_{e,-} = \begin{pmatrix} \phi_2,\phi_2 & \phi_2,\phi_4 & \phi_2,\bar{\Pi}^{\mathrm{l}}_{33} & \phi_2,\bar{\Pi}^{\mathrm{s}}_{33} & \phi_2,\bar{\Pi}^{\mathrm{l}}_{88} & \phi_2,\bar{\Pi}^{\mathrm{s}}_{88} \\ \vdots & \phi_4,\phi_4 & \phi_4,\bar{\Pi}^{\mathrm{l}}_{33} & \phi_4,\bar{\Pi}^{\mathrm{s}}_{33} & \phi_4,\bar{\Pi}^{\mathrm{l}}_{88} & \phi_4,\bar{\Pi}^{\mathrm{s}}_{88} \\ \vdots & \vdots & \bar{\Pi}^{\mathrm{l}}_{33},\bar{\Pi}^{\mathrm{l}}_{33} & \bar{\Pi}^{\mathrm{l}}_{33},\bar{\Pi}^{\mathrm{s}}_{33} & \bar{\Pi}^{\mathrm{l}}_{33},\bar{\Pi}^{\mathrm{l}}_{88} & \bar{\Pi}^{\mathrm{l}}_{33},\bar{\Pi}^{\mathrm{s}}_{88} \\ \vdots & \vdots & \vdots & \bar{\Pi}^{\mathrm{s}}_{33},\bar{\Pi}^{\mathrm{s}}_{33} & \bar{\Pi}^{\mathrm{s}}_{33},\bar{\Pi}^{\mathrm{l}}_{88} & \bar{\Pi}^{\mathrm{s}}_{33},\bar{\Pi}^{\mathrm{s}}_{88} \\ \vdots & \vdots & \vdots & \vdots & \bar{\Pi}^{\mathrm{l}}_{88},\bar{\Pi}^{\mathrm{l}}_{88} & \bar{\Pi}^{\mathrm{l}}_{88},\bar{\Pi}^{\mathrm{s}}_{88} \\ \dots & \dots & \dots & \dots & \dots & \bar{\Pi}^{\mathrm{s}}_{88},\bar{\Pi}^{\mathrm{s}}_{88} \end{pmatrix}_e$$

r and Cov for $SU(3)_f$-symmetric ensembles

The residue vector is defined as

$$r_{e,i} = \begin{pmatrix} \phi_2 \\ \bar{\Pi}(a, \phi_2, 3\phi_2/2; d = \mathrm{l}, i) \\ \bar{\Pi}(a, \phi_2, 3\phi_2/2; d = \mathrm{s}, i) \end{pmatrix} - \begin{pmatrix} \phi_2 \\ \bar{\Pi}_i^{\mathrm{l}} \\ \bar{\Pi}_i^{\mathrm{s}} \end{pmatrix}_e ,$$

where e runs over the ensembles data. The index structure of the covariance matrix is

$$\mathrm{Cov}_{e,i} = \begin{pmatrix} \phi_2, \phi_2 & \phi_2, \bar{\Pi}_i^{\mathrm{l}} & \phi_2, \bar{\Pi}_i^{\mathrm{s}} \\ \vdots & \bar{\Pi}_i^{\mathrm{l}}, \bar{\Pi}_i^{\mathrm{l}} & \bar{\Pi}_i^{\mathrm{l}}, \bar{\Pi}_i^{\mathrm{s}} \\ \dots & \dots & \bar{\Pi}_i^{\mathrm{s}}, \bar{\Pi}_i^{\mathrm{s}} \end{pmatrix}_e$$

Jacobian

We define a vector y of length $m \times 1$ containing all the fit parameters,

$$y \equiv (\bar{\Pi}^{\mathrm{sym}},\ \alpha_{2,\mathrm{S}},\ \alpha_{3,\mathrm{S}},\ \beta_{1,33},\ \text{etc.})$$

The vector y includes ϕ_2 for the SU(3)$_\mathrm{f}$-symmetric ensembles, and ϕ_2 and ϕ_4 for the rest.
Then, we apply the Cholesky decomposition on $\chi^2_{e,-}$, $\chi^2_{e,33}$, χ^2_{88},

$$\chi_{e,.} = L^{-1}_{e,.} r_{e,.},$$

such that $\chi_{e,.}$ is a $n \times 1$ vector, with n the number of dependent ($\bar{\Pi}$) plus independent (ϕ_2, ϕ_4) variables for a given ensemble.
Then, we compute the $m \times n$ matrix of derivatives

$$\left(\frac{\partial \chi_{e,.}}{\partial y}\right)^T = L^{-1}_{e,.}\left(\frac{\partial r_{e,.}}{\partial y}\right)^T,$$

For SU(3)$_\mathrm{f}$-symmetric ensembles, $m = 10$ and $n = 3$, while $m = 11$ and $n = 6$ for the rest. Then, the Jacobian for every ensemble is [40]

$$\frac{\partial \chi_e}{\partial y}\chi_e = \begin{cases} \frac{\partial \chi_{e,-}}{\partial y}\chi_{e,-}, & \text{if } M_{\pi,e} \neq M_{K,e} \\ \frac{1}{2}\left(\frac{\partial \chi_{e,\mathbf{33}}}{\partial y}\chi_{e,33} + \frac{\partial \chi_{e,\mathbf{88}}}{\partial y}\chi_{e,88}\right), & \text{if } M_{\pi,e} = M_{K,e}. \end{cases}$$

Lattice spacing dependence

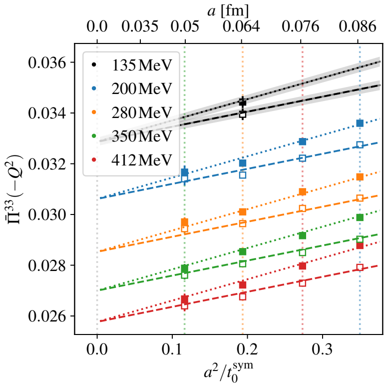

Smooth step function between a^2 and $a^2 + a^3$

$$\Theta(Q^2) = 0.5\left(1 + \tanh\left((Q^2 - 2.5\,\mathrm{GeV}^2)/1.0\,\mathrm{GeV}^2\right)\right)$$

Logarithmic corrections to the a^2 behaviour [41]

$$\tilde{c}_{\bar{\Pi}}(Q^2) \cdot (a^2/t_0^{\mathrm{sym}}) \log(t_0^{\mathrm{sym}}/a^2)/2 \sim 0$$

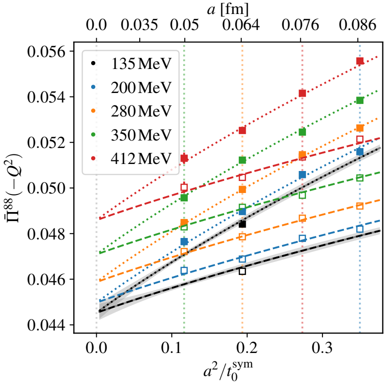

Scale-setting uncertainty

Dominant uncertainty for $0 < Q^2 \lesssim 3\,\mathrm{GeV}^2$

Although $\bar{\Pi}$ is dimensionsless, the scale enters indirectly through

- The virtuality $8t_0 Q^2$ in the kernel $K(t, Q^2)$ of the TMR
- The physical point definition ϕ_2^{phy}, ϕ_4^{phy}

Using linear error propagation, the relative error of $\bar{\Pi}$ is

$$\frac{\Delta\bar{\Pi}}{\bar{\Pi}} \approx \left| \frac{2 l_0^2 Q^2}{\bar{\Pi}} \frac{\partial\bar{\Pi}}{\partial l_0^2 Q^2} + \frac{2\phi_2^{\text{phy}}}{\bar{\Pi}} \frac{\partial\bar{\Pi}}{\partial\phi_2^{\text{phy}}} + \frac{2\phi_4^{\text{phy}}}{\bar{\Pi}} \frac{\partial\bar{\Pi}}{\partial\phi_4^{\text{phy}}} \right| \frac{\Delta l_0}{l_0}$$

- The first term is positive, and varies with Q^2
- The second and third terms are negative
- $\Delta\bar{\Pi}/\bar{\Pi} \sim 0$ in some cases

$\rightarrow$ We use bootstrap sampling instead

Scale setting: $l_0 \equiv \sqrt{8t_0} = 0.415\ (4)\ (2)$ fm [12]

Improved determination in progress

Isospin breaking effects [45, 35, 46]

Evaluate quark-connected $\bar{\Pi}$ in QCD + QED at $M_\pi \sim 220\,\mathrm{MeV}$ → Estimate relative size of isospin breaking effects → Add to error budget

- → Non-compact $\mathrm{QED_L}$-action for IR regularisation, Coulomb gauge [42]
- → Same boundary conditions for the photon and gluon fields
- → Reweighting and leading perturbative expansion in $\Delta\epsilon = \epsilon - \epsilon^{(0)}$ around $\epsilon^{(0)}$, where

  QCD + QED parametrised by $\epsilon = \left(M_u, M_d, M_s, \beta, e^2\right)$

  $\mathrm{QCD_{iso}}$ parametrised by $\epsilon^{(0)} = (M_{ud}^{(0)}, M_{ud}^{(0)}, M_s^{(0)}, \beta^{(0)}, 0)$

  [43, 44]
- → Neglect IB effects in the scale
- → Renormalisation scheme: Match QCD + QED and $\mathrm{QCD_{iso}}$ using

$$M^2_{\pi^0} \propto M_u + M_d$$

$$M^2_{K^+} - M^2_{K^0} - M^2_{\pi^+} + M^2_{\pi^0} \propto M_u - M_d$$

$$M^2_{K^+} + M^2_{K^0} - M^2_{\pi^+} \propto M_s$$

Missing quark contributions

The charm-quark contribution is determined from the quark-connected component alone. Therefore, there are two missing effects:

- ➔ Valence charm-quark loops

  [16] reports this contribution to be $< 1\%$ of the u, d, s quark-disconnected contribution to a_μ^{HVP} → 0.1‰ effect we neglect

- ➔ Sea charm-quark loops

  To estimate the effect of quenching, we employ a phenomenological estimate,

  Split $\bar{\Pi}$ into two parts,

$$\bar{\Pi}(-Q_0^2) = \underbrace{\left[\bar{\Pi}(-Q_0^2) - \bar{\Pi}(-1\,\mathrm{GeV}^2)\right]}_{①} + \underbrace{\bar{\Pi}(-1\,\mathrm{GeV}^2)}_{②}$$

① Charm sea-quark effects appear at $\mathcal{O}\left(\alpha_s^2\right)$ in perturbation theory → negligible

② D^+D^-, $D^0\bar{D}^0$, $D_s^+D_s^-$ contribute to the (u, d, s) vector correlators.
Using scalar-QED → 3‰ effect added to error budget

The bottom-quark contribution is determined by [15] → maximum 3‰ effect added to error budget to compare with phenomenology

Relating $\bar{\Pi}$ and the Stieltjes function

The integral representation of a Stieltjes function $\Phi(z)$ is [47, 48],

$$\Phi(z) = \int_0^{1/R} \frac{\mathrm{d}\nu(\tau)}{1+\tau z},$$

where $\nu(z)$ is real, bounded, non-decreasing on the interval $[0, 1/R]$, and takes infinitely many values on that said interval. $\Phi(z)$ is analytic in the entire complex plane except on the cut $z \in (-\infty, -R]$, and decreases monotonically in the range $z \in (-R, \infty)$.Choosing [48]

$$\tau = \frac{1}{s}, \qquad \mathrm{d}\nu(\tau) = \mathrm{d}\tau\ \rho(1/\tau),$$

$$R = 4M_\pi^2, \qquad \rho(1/\tau) = \frac{1}{\pi}\mathrm{Im}\Pi(1/\tau),$$

we see that $\bar{\Pi}$ is a Stieltjes function [48],

$$\bar{\Pi}(-Q^2) = Q^2\Phi(Q^2), \qquad \Phi(Q^2) = \int_{4M_\pi^2}^{\infty} \mathrm{d}s\ \frac{\rho(s)}{s(s+Q^2)}.$$

The spectral function $\rho(s)$ is non-negative in the integration range.

Relating the Stieltjes function and the Padé approximants (PAs)

A Padé approximant $R_M^N(Q^2)$ is the ratio of two polynomials of degrees N and M [49],

$$R_M^N(Q^2) = \frac{\sum_{n=0}^{N} a_n Q^{2n}}{1 + \sum_{m=1}^{M} b_m Q^{2m}}$$

To build Padé approximants (PAs) to describe $\Phi(Q^2)$, we employ the following theorem [49, 50]: Given P points $(Q_i^2, \Phi(Q_i^2))$, $i \in \{1, \ldots, \mathrm{P}\}$, a sequence of Padé approximants can be constructed converging to $\Phi(Q^2)$ in the limit $\mathrm{P} \to \infty$ on any closed, bounded region of the complex plane, excluding the cut $Q^2 \in (-\infty, -4M_\pi^2]$. Then, the Stieltjes function $\Phi(Q^2)$ can be built as a continued fraction [49],

$$\Phi(Q^2) = \cfrac{\psi_1(Q_1^2)}{1 + \cfrac{(Q^2 - Q_1^2)\ \psi_2(Q_2^2)}{1 + \cfrac{(Q^2 - Q_2^2)\ \psi_3(Q_3^2)}{\ddots 1 + (Q^2 - Q_{\mathrm{P}-1}^2)\ \psi_{\mathrm{P}}(Q_{\mathrm{P}}^2)}}}.$$

The functions ψ_i can be constructed recursively using [51]

$$\psi_1 = \Phi(Q_1^2), \qquad \psi_i(Q^2) = \frac{\psi_{i-1}(Q_{i-1}^2) - \psi_{i-1}(Q_i^2)}{(Q^2 - Q_{i-1}^2)\psi_{i-1}(Q^2)}, \qquad i > 1.$$

[1] P. A. Zyla et al. "Review of Particle Physics". In: *PTEP* 2020.8 (2020), p. 083C01. DOI: 10.1093/ptep/ptaa104.

[2] Christian Sturm. "Leptonic contributions to the effective electromagnetic coupling at four-loop order in QED". In: *Nuclear Physics B* 874.3 (2013), pp. 698–719. ISSN: 0550-3213. DOI: https://doi.org/10.1016/j.nuclphysb.2013.06.009. URL: https://www.sciencedirect.com/science/article/pii/S0550321313003234.

[3] M. Steinhauser. "Leptonic contribution to the effective electromagnetic coupling constant up to three loops". In: *Phys. Lett. B* 429 (1998), pp. 158–161. DOI: 10.1016/S0370-2693(98)00503-6. arXiv: hep-ph/9803313.

[4] Alexander Keshavarzi, Daisuke Nomura, and Thomas Teubner. "$g-2$ of charged leptons, $\alpha(M_Z^2)$, and the hyperfine splitting of muonium". In: *Phys. Rev. D* 101.1 (2020), p. 014029. DOI: 10.1103/PhysRevD.101.014029. arXiv: 1911.00367 [hep-ph].

[5] K. G. Chetyrkin, Johann H. Kuhn, and M. Steinhauser. "Three loop polarization function and O (alpha-s**2) corrections to the production of heavy quarks". In: *Nucl. Phys. B* 482 (1996), pp. 213–240. DOI: 10.1016/S0550-3213(96)00534-2. arXiv: hep-ph/9606230.

[6] S. Eidelman et al. "Testing nonperturbative strong interaction effects via the Adler function". In: *Phys. Lett. B* 454 (1999), pp. 369–380. DOI: 10.1016/S0370-2693(99)00389-5. arXiv: hep-ph/9812521.

[7] F. Jegerlehner. "Hadronic effects in (g - 2)(mu) and alpha(QED)(M(Z)): Status and perspectives". In: *4th International Symposium on Radiative Corrections: Applications of Quantum Field Theory to Phenomenology*. Jan. 1999, pp. 75–89. arXiv: hep-ph/9901386.

[8] F. Jegerlehner. "The Running fine structure constant alpha(E) via the Adler function". In: *Nucl. Phys. B Proc. Suppl.* 181-182 (2008). Ed. by Cesare Bini and Graziano Venanzoni, pp. 135–140. DOI: 10.1016/j.nuclphysbps.2008.09.010. arXiv: 0807.4206 [hep-ph].

[9] F. Jegerlehner. "$\alpha_{QED,eff}(s)$ for precision physics at the FCC-ee/ILC". In: *CERN Yellow Reports: Monographs* 3 (2020). Ed. by A. Blondel et al., pp. 9–37. DOI: 10.23731/CYRM-2020-003.9.

[10] D. Bernecker and H. B. Meyer. "Vector correlators in lattice QCD: Methods and applications". In: *European Physical Journal A* 47, 148 (Nov. 2011), p. 148. DOI: 10.1140/epja/i2011-11148-6. arXiv: 1107.4388 [hep-lat].

[11] A. Francis et al. "New representation of the Adler function for lattice QCD". In: *prd* 88.5, 054502 (Sept. 2013), p. 054502. DOI: 10.1103/PhysRevD.88.054502. arXiv: 1306.2532 [hep-lat].

[12] Mattia Bruno, Tomasz Korzec, and Stefan Schaefer. "Setting the scale for the CLS $2+1$ flavor ensembles". In: *Phys. Rev. D* 95.7 (2017), p. 074504. DOI: 10.1103/PhysRevD.95.074504. arXiv: 1608.08900 [hep-lat].

[13] Antoine Gérardin et al. "The leading hadronic contribution to $(g-2)_\mu$ from lattice QCD with $N_\mathrm{f} = 2+1$ flavours of O(a) improved Wilson quarks". In: *Phys. Rev. D* 100.1 (2019), p. 014510. DOI: 10.1103/PhysRevD.100.014510. arXiv: 1904.03120 [hep-lat].

[14] Mattia Bruno et al. "Simulation of QCD with $N_f = 2 + 1$ flavors of non-perturbatively improved Wilson fermions". In: *JHEP* 02 (2015), p. 043. DOI: 10.1007/JHEP02(2015)043. arXiv: 1411.3982 [hep-lat].

[15] B. Colquhoun et al. "Υ and Υ' Leptonic Widths, a_μ^b and m_b from full lattice QCD". In: *Phys. Rev. D* 91.7 (2015), p. 074514. DOI: 10.1103/PhysRevD.91.074514. arXiv: 1408.5768 [hep-lat].

[16] Sz. Borsanyi et al. "Hadronic vacuum polarization contribution to the anomalous magnetic moments of leptons from first principles". In: *Phys. Rev. Lett.* 121.2 (2018), p. 022002. DOI: 10.1103/PhysRevLett.121.022002. arXiv: 1711.04980 [hep-lat].

[17] Maxwell T. Hansen and Agostino Patella. "Finite-volume and thermal effects in the leading-HVP contribution to muonic $(g-2)$". In: *JHEP* 2010.10 (Oct. 2020), p. 029. DOI: 10.1007/jhep10(2020)029. arXiv: 2004.03935 [hep-lat].

[18] Maxwell T. Hansen and Agostino Patella. "Finite-volume effects in $(g-2)_\mu^{\text{HVP,LO}}$". In: *Phys. Rev. Lett.* 123 (2019), p. 172001. DOI: 10.1103/PhysRevLett.123.172001. arXiv: 1904.10010 [hep-lat].

[19] Meyer. "Lattice QCD and the Timelike Pion Form Factor". In: *Phys. Rev. Lett.* 107 (2011), p. 072002. DOI: 10.1103/PhysRevLett.107.072002. arXiv: 1105.1892 [hep-lat].

[20] M. Della Morte et al. "The hadronic vacuum polarization contribution to the muon $g-2$ from lattice QCD". In: *ArXiv e-prints* (May 2017). arXiv: 1705.01775 [hep-lat].

[21] Laurent Lellouch and Martin Luscher. "Weak transition matrix elements from finite volume correlation functions". In: *Commun. Math. Phys.* 219 (2001), pp. 31–44. DOI: 10.1007/s002200100410. arXiv: hep-lat/0003023.

[22] R. L. Workman et al. "Review of Particle Physics". In: *PTEP* 2022 (2022), p. 083C01. DOI: 10.1093/ptep/ptac097.

[23] G. Colangelo et al. "Prospects for precise predictions of a_μ in the Standard Model". In: (Mar. 2022). arXiv: 2203.15810 [hep-ph].

[24] Sz. Borsanyi et al. "Leading hadronic contribution to the muon magnetic moment from lattice QCD". In: *Nature* 593.7857 (2021), pp. 51–55. DOI: 10.1038/s41586-021-03418-1. arXiv: 2002.12347 [hep-lat].

[25] T. Blum et al. "Calculation of the hadronic vacuum polarization contribution to the muon anomalous magnetic moment". In: *Phys. Rev. Lett.* 121.2 (2018), p. 022003. DOI: 10.1103/PhysRevLett.121.022003. arXiv: 1801.07224 [hep-lat].

[26] G. Colangelo et al. "Data-driven evaluations of Euclidean windows to scrutinize hadronic vacuum polarization". In: *Phys. Lett. B* 833 (2022), p. 137313. DOI: 10.1016/j.physletb.2022.137313. arXiv: 2205.12963 [hep-ph].

[27] J. Benesch et al. "The MOLLER Experiment: An Ultra-Precise Measurement of the Weak Mixing Angle Using M\oller Scattering". In: (Nov. 2014). arXiv: 1411.4088 [nucl-ex].

[28] Y. X. Zhao. "Parity Violation in Deep Inelastic Scattering with the SoLID Spectrometer at JLab". In: *22nd International Symposium on Spin Physics*. Jan. 2017. arXiv: 1701.02780 [nucl-ex].

[29] Dominik Becker et al. "The P2 experiment". In: *Eur. Phys. J. A* 54.11 (2018), p. 208. DOI: 10.1140/epja/i2018-12611-6. arXiv: 1802.04759 [nucl-ex].

[30] Antoine Gerardin, Tim Harris, and Harvey B. Meyer. "Nonperturbative renormalization and $O(a)$-improvement of the nonsinglet vector current with $N_f = 2+1$ Wilson fermions and tree-level Symanzik improved gauge action". In: *Phys. Rev. D* 99.1 (2019), p. 014519. DOI: 10.1103/PhysRevD.99.014519. arXiv: 1811.08209 [hep-lat].

[31] Marco Cè et al. "The hadronic running of the electromagnetic coupling and the electroweak mixing angle from lattice QCD". In: *JHEP* 08 (2022), p. 220. DOI: 10.1007/JHEP08(2022)220. arXiv: 2203.08676 [hep-lat].

[32] Jochen Heitger and Fabian Joswig. "The renormalised $\mathrm{O}(a)$ improved vector current in three-flavour lattice QCD with Wilson quarks". In: *Eur. Phys. J. C* 81.3 (2021), p. 254. DOI: 10.1140/epjc/s10052-021-09037-4. arXiv: 2010.09539 [hep-lat].

[33] Patrick Fritzsch. "Mass-improvement of the vector current in three-flavor QCD". In: *JHEP* 06 (2018), p. 015. DOI: 10.1007/JHEP06(2018)015. arXiv: 1805.07401 [hep-lat].

[34] Ulli Wolff. "Monte Carlo errors with less errors". In: *Comput. Phys. Commun.* 156 (2004). [Erratum: Comput.Phys.Commun. 176, 383 (2007)], pp. 143–153. DOI: 10.1016/S0010-4655(03)00467-3. arXiv: hep-lat/0306017.

[35] Andreas Risch. "Isospin breaking effects in hadronic matrix elements on the lattice". eng. PhD thesis. Mainz, 2021. DOI: http://doi.org/10.25358/openscience-6314.

[36] Barbara De Palma et al. "A Python program for the implementation of the Γ -method for Monte Carlo simulations". In: *Comput. Phys. Commun.* 234 (2019), pp. 294–301. DOI: 10.1016/j.cpc.2018.07.004. arXiv: 1703.02766 [hep-lat].

[37] T. Blum et al. *Discussion: criteria for inclusion in WP update at the last g-2 theory initiative workshop, Wed 30/06 at 15:05 CEST*. 2021. URL: https://agenda.hepl.phys.nagoya-u.ac.jp/indico/conferenceDisplay.py?ovw=True&confId=1691.

[38] Ananth Ranganathan. "The levenberg-marquardt algorithm". In: *Tutoral on LM algorithm* 11.1 (2004), pp. 101–110.

[39] Pauli Virtanen et al. "SciPy 1.0: Fundamental Algorithms for Scientific Computing in Python". In: *Nature Methods* 17 (2020), pp. 261–272. DOI: 10.1038/s41592-019-0686-2.

[40] Darrell A. Turkington. "New Matrix Calculus Results". In: *Generalized Vectorization, Cross-Products, and Matrix Calculus*. Cambridge University Press, 2013, pp. 164–213. DOI: 10.1017/CBO9781139424400.006.

[41] Marco Cè et al. "Vacuum correlators at short distances from lattice QCD". In: (June 2021). arXiv: 2106.15293 [hep-lat].

[42] Masashi Hayakawa and Shunpei Uno. "QED in finite volume and finite size scaling effect on electromagnetic properties of hadrons". In: *Prog. Theor. Phys.* 120 (2008), pp. 413–441. DOI: 10.1143/PTP.120.413. arXiv: 0804.2044 [hep-ph].

[43] G. M. de Divitiis et al. "Isospin breaking effects due to the up-down mass difference in Lattice QCD". In: *JHEP* 04 (2012), p. 124. DOI: 10.1007/JHEP04(2012)124. arXiv: 1110.6294 [hep-lat].

[44] G. M. de Divitiis et al. "Leading isospin breaking effects on the lattice". In: *Phys. Rev. D* 87.11 (2013), p. 114505. DOI: 10.1103/PhysRevD.87.114505. arXiv: 1303.4896 [hep-lat].

[45] Andreas Risch and Hartmut Wittig. "Leading isospin breaking effects in the HVP contribution to a_μ and to the running of α". In: *PoS* LATTICE2021 (2022), p. 106. DOI: 10.22323/1.396.0106. arXiv: 2112.00878 [hep-lat].

[46] Andreas Risch and Hartmut Wittig. "Leading isospin breaking effects in the hadronic vacuum polarisation with open boundaries". In: *PoS* LATTICE2019 (2019), p. 296. DOI: 10.22323/1.363.0296. arXiv: 1911.04230 [hep-lat].

[47] Jacques Hadamard. *Essai sur l'étude des fonctions, données par leur développement de Taylor*. Gauthier-Villars, 1892.

[48] Christopher Aubin et al. "Model-independent parametrization of the hadronic vacuum polarization and g-2 for the muon on the lattice". In: *Phys. Rev. D* 86 (2012), p. 054509. DOI: 10.1103/PhysRevD.86.054509. arXiv: 1205.3695 [hep-lat].

[49] Michael Barnsley. "The bounding properties of the multipoint Padé approximant to a series of Stieltjes on the real line". In: *Journal of Mathematical Physics* 14.3 (1973), pp. 299–313. DOI: 10.1063/1.1666314. eprint: https://doi.org/10.1063/1.1666314. URL: https://doi.org/10.1063/1.1666314.

[50] George A. Baker. "Best Error Bounds for Padé Approximants to Convergent Series of Stieltjes". In: *Journal of Mathematical Physics* 10.5 (1969), pp. 814–820. DOI: 10.1063/1.1664911. eprint: https://doi.org/10.1063/1.1664911. URL: https://doi.org/10.1063/1.1664911.

[51] G. A. Baker. “Best error bounds for pade approximants to convergent series of stieltjes”. In: *J. Math. Phys.* 10 (1969), pp. 814–820. DOI: 10.1063/1.1664911.